JOURNAL OF GUIDANCE, CONTROL, AND DYNAMICS
Vol. 28, No. 6, November–December 2005

Engineering Notes

ENGINEERING NOTES are short manuscripts describing new developments or important results of a preliminary nature. These Notes should not exceed 2500 words (where a figure or table counts as 200 words). Following informal review by the Editors, they may be published within a few months of the date of receipt. Style requirements are the same as for regular contributions (see inside back cover).

Analytic Orbital Averaging Technique for Computing Tangential-Thrust Trajectories

Y. Gao* and C. A. Kluever†
University of Missouri–Columbia, Columbia, Missouri 65211

Introduction

An attractive characteristic of tangential thrust (aligning the thrust and velocity vectors) is that it provides the most efficient strategy for changing the instantaneous orbital energy rate of a low-thrust spacecraft. Therefore, tangent thrust is often proposed for orbit raising,[1] planetary escape,[2] or planetary capture maneuvers.[3] Low tangential-thrust trajectories are slowly developing spirals about the attracting body, which may result in hundreds or thousands of orbital revolutions with current electric propulsion technology. Therefore, simulating many-revolution, long-duration trajectories using precise numerical integration methods is very time consuming. In the 1950s and 1960s, Perkins,[4] Stark and Arthur,[5] and Zee[6] all developed analytic solutions for analyzing and computing low-thrust trajectories using a constant, continuous tangential acceleration in a two-body gravity field. Kechichian[1] developed an averaging method for orbital raising using tangential acceleration for small-to-moderate eccentricity orbits. Kechichian also considered the Earth-shadow effect (periods of zero thrust for a solar-electric device) in his analysis. Sukhanov and Prado[7] developed an approximate method to change spacecraft energy in minimum time using low tangential acceleration near an oblate planet without considering the shadow effect.

In this Note, an analytic orbital averaging technique is developed for computing long-duration low tangential-thrust trajectories. Analytic expressions for the incremental changes in classical orbital elements for each orbital revolution are obtained by using simple approximations, and these expressions lead to relatively simple formulations. Our technique accommodates the mass flow rate (varying thrust acceleration), Earth-shadow and Earth-oblateness effects, and initial high-eccentricity orbits. Furthermore, the time histories of the mean values of the non-secular classical orbital elements are obtained. Our orbital averaging technique provides a fast algorithm for simulating many-revolution trajectories using low tangential acceleration and also exhibits favorable accuracy compared with simulation results obtained by precise numerical integration methods.

Received 19 November 2004; revision received 15 February 2005; accepted for publication 21 February 2005. Copyright © 2005 by the American Institute of Aeronautics and Astronautics, Inc. All rights reserved. Copies of this paper may be made for personal or internal use, on condition that the copier pay the $10.00 per-copy fee to the Copyright Clearance Center, Inc., 222 Rosewood Drive, Danvers, MA 01923; include the code 0731-5090/05 $10.00 in correspondence with the CCC.

*Postdoctoral Research Fellow, Mechanical and Aerospace Engineering Department.
†Professor, Mechanical and Aerospace Engineering Department. Associate Fellow AIAA.

Orbital Averaging Technique

To obtain the new orbital averaging technique, we start with the variational form of the classical orbital elements[8] for planar maneuvers (no out-of-plane thrust component):

$$\frac{\mathrm{d}a}{\mathrm{d}t} = \frac{2a^2 e \sin\theta}{h} f_r + \frac{2a^2 p}{hr} f_\theta \tag{1}$$

$$\frac{\mathrm{d}e}{\mathrm{d}t} = \frac{1}{h} p \sin\theta f_r + \frac{1}{h}[(p+r)\cos\theta + re] f_\theta \tag{2}$$

$$\frac{\mathrm{d}\omega}{\mathrm{d}t} = -\frac{p\cos\theta}{he} f_r + \frac{(p+r)\sin\theta}{he} f_\theta \tag{3}$$

$$\frac{\mathrm{d}E}{\mathrm{d}t} = \frac{na}{r} + \frac{1}{nae}\left[f_r(\cos\theta - e) - f_\theta\left(1 + \frac{r}{a}\right)\sin\theta \right] \tag{4}$$

where a is the semimajor axis, e is the eccentricity, ω is the argument of the periapsis, θ is the true anomaly, E is the eccentric anomaly, $p = a(1-e^2)$ is the semilatus rectum, $h = \sqrt{(\mu p)}$ is the angular momentum, $n = \sqrt{(\mu/a^3)}$ is the mean motion, and $r = p/(1+e\cos\theta)$ is the orbital radius. The variable μ denotes the gravitational parameter of the attracting body. Radial and circumferential thrust-acceleration components are f_r and f_θ, respectively. Because the thrust accelerations f_r and f_θ are much smaller than the gravitational acceleration, Eq. (4) can be approximated as

$$\frac{\mathrm{d}E}{\mathrm{d}t} \approx \frac{na}{r} \tag{5}$$

Further explanation of the assumption that leads to Eq. (5) is in order. For nearly circular orbits, the first term in Eq. (4) is approximately n, whereas the second factor $(1/nae)$ is not necessarily small. However, when thrust acceleration magnitude is very small, it essentially cancels the effect of the $1/e$ term. For example, if $e = 0.001$ and $a = 1.05$ Earth radii (nearly circular low Earth orbit) and $f = 10^{-5}$ m/s^2, then the second term in Eq. (4) is two orders of magnitude smaller than the first term.

The relationship between true and eccentric anomalies is given by

$$\sin\theta = \frac{\sin E\sqrt{1-e^2}}{1 - e\cos E}, \qquad \cos\theta = \frac{\cos E - e}{1 - e\cos E} \tag{6}$$

Therefore, derivatives of the classical orbital elements, a, e, and ω, with respect to eccentric anomaly E can be obtained by dividing Eqs. (1–3) by Eq. (5),

$$\frac{\mathrm{d}a}{\mathrm{d}E} = \frac{2a^3}{\mu}\left(f_r e \sin E + f_\theta\sqrt{1-e^2} \right) \tag{7}$$

$$\frac{\mathrm{d}e}{\mathrm{d}E} = \frac{a^2}{\mu}\left[f_r(1-e^2)\sin E + f_\theta(2\cos E - e - e\cos^2 E)\sqrt{1-e^2} \right] \tag{8}$$

$$\frac{\mathrm{d}\omega}{\mathrm{d}E} = -\frac{a^2}{e\mu}\left[f_r(\cos E - e)\sqrt{1-e^2} - f_\theta(2 - e^2 - e\cos E)\sin E \right] \tag{9}$$

The radial and circumferential components for tangential acceleration can be expressed as

$$f_r = f\frac{e\sin E}{\sqrt{1-e^2\cos^2 E}} \tag{10}$$

$$f_\theta = f\frac{\sqrt{1-e^2}}{\sqrt{1-e^2\cos^2 E}} \tag{11}$$

where $f=\sqrt{(f_r^2+f_\theta^2)}$. If we assume that a, e, ω, and f are constant over an orbital revolution, then the incremental changes in the elements due to tangential thrust over an orbital arc from E_0 to E_f can be obtained by integrating Eqs. (7–9) with thrust components (10) and (11),

$$\int_{E_0}^{E_f}\frac{\mathrm{d}a}{\mathrm{d}E}\,\mathrm{d}E = \frac{2a^3}{\mu}f\int_{E_0}^{E_f}\sqrt{1-e^2\cos^2 E}\,\mathrm{d}E \tag{12}$$

$$\int_{E_0}^{E_f}\frac{\mathrm{d}e}{\mathrm{d}E}\,\mathrm{d}E = \frac{2a^2}{e\mu}(1-e^2)f \times\left\{\begin{aligned}&\int_{E_0}^{E_f}\left(\sqrt{1-e^2\cos^2 E}-\frac{1}{\sqrt{1-e^2\cos^2 E}}\right)\mathrm{d}E\\&+\left[\ell_n\left(\sin E+\frac{1}{e}\sqrt{1-e^2\cos^2 E}\right)\right]_{E_0}^{E_f}\end{aligned}\right\} \tag{13}$$

$$\int_{E_0}^{E_f}\frac{\mathrm{d}\omega}{\mathrm{d}E}\,\mathrm{d}E = -\frac{2a^2}{e^2\mu}\sqrt{1-e^2}f \times\left[\sqrt{1-e^2\cos^2 E}+\sin^{-1}(e\cos E)\right]_{E_0}^{E_f} \tag{14}$$

Note that we are unable to find analytic expressions for the terms

$$\int_{E_0}^{E_f}\sqrt{1-e^2\cos^2 E}\,\mathrm{d}E$$

$$\int_{E_0}^{E_f}\left(\sqrt{1-e^2\cos^2 E}-\frac{1}{\sqrt{1-e^2\cos^2 E}}\right)\mathrm{d}E$$

in Eqs. (12) and (13). However, we can utilize the following approximations for the integrands of these two terms:

$$\sqrt{1-e^2\cos^2 E}\approx\sqrt{1-e^2}+\left(1-\sqrt{1-e^2}\right)\sin^2 E \tag{15}$$

$$\sqrt{1-e^2\cos^2 E}-\frac{1}{\sqrt{1-e^2\cos^2 E}} = \frac{-e^2\cos^2 E}{\sqrt{1-e^2\cos^2 E}}\approx\frac{-e^2\cos^2 E}{\sqrt{1-e^2c}} \tag{16}$$

In Eq. (15), we use a simple periodic function (including the term $\sin^2 E$) with the same boundaries by determining the lower and upper limits of the term $\sqrt{(1-e^2\cos^2 E)}$. In Eq. (16), a simple local approximation is used by converting the bounded function $\cos^2 E$ to a constant parameter c that is between 0 and 1. (Numerical trials for a range $c\in[0,1]$ showed that $c=0.8$ yielded satisfactory accuracy.) The approximations exhibit satisfactory accuracy, and for near-circular orbits, the approximation becomes more accurate and the selected value for constant c is less important. The analytic integrals of the approximate integrands [Eqs. (15) and (16)] are

$$\int_{E_0}^{E_f}\sqrt{1-e^2\cos^2 E}\,\mathrm{d}E \approx\left[\sqrt{1-e^2}E+\left(1-\sqrt{1-e^2}\right)(0.5E-0.25\sin 2E)\right]_{E_0}^{E_f} \tag{17}$$

$$\int_{E_0}^{E_f}\left(\sqrt{1-e^2\cos^2 E}-\frac{1}{\sqrt{1-e^2\cos^2 E}}\right)\mathrm{d}E \approx\frac{-e^2}{\sqrt{1-e^2c}}[0.5E+0.25\sin 2E]_{E_0}^{E_f} \tag{18}$$

The averaged changes of the orbital elements due to oblateness (J_2) perturbations are

$$\frac{\mathrm{d}\bar{a}}{\mathrm{d}t}=\frac{\mathrm{d}\bar{e}}{\mathrm{d}t}=\frac{\mathrm{d}\bar{i}}{\mathrm{d}t}=0 \tag{19}$$

$$\frac{\mathrm{d}\bar{\Omega}}{\mathrm{d}t}=-\frac{3}{2}J_2\frac{r_e^2}{a^2(1-e^2)^2}n\cos i \tag{20}$$

$$\frac{\mathrm{d}\bar{\omega}}{\mathrm{d}t}=\frac{3}{4}J_2\frac{r_e^2}{a^2(1-e^2)^2}n(5\cos^2 i-1) \tag{21}$$

where i is inclination, Ω is longitude of the ascending node, and r_e is the Earth radius ($r_e=1$ Re $=6378.14$ km). The overbar denotes averaged elements with respect to J_2 effects. With use of the notation $\boldsymbol{x}_A=[a,e,i,\Omega,\omega]^T$ for the averaged elements due to in-plane thrust-acceleration perturbations and $\bar{\boldsymbol{x}}=[\bar{a},\bar{e},\bar{i},\bar{\Omega},\bar{\omega}]^T$ for the averaged elements due to J_2 perturbations, the total incremental changes in the classical orbital elements with respect to both effects for the next k revolutions are computed as

$$\Delta\boldsymbol{x}=\left[\int_{E_{\mathrm{ex}}}^{E_{\mathrm{en}}}\frac{\mathrm{d}\boldsymbol{x}_A}{\mathrm{d}E}\,\mathrm{d}E+\frac{\mathrm{d}\bar{\boldsymbol{x}}}{\mathrm{d}t}\frac{2\pi}{n}\right]k \tag{22}$$

where E_{en} and E_{ex} are Earth-shadow entrance and exit eccentric anomalies, respectively. The mass loss Δm and flight time Δt every k revolutions are

$$\Delta m=-\left[2\eta P\Big/\left(gI_{\mathrm{sp}}\right)^2\right][(1/n)(E_{\mathrm{en}}-e\sin E_{\mathrm{en}} -E_{\mathrm{ex}}+e\sin E_{\mathrm{ex}})]k \tag{23}$$

$$\Delta t=(2\pi/n)k \tag{24}$$

where P is input power, I_{sp} is specific impulse, η is engine efficiency, and g is sea-level Earth gravitational acceleration. Thrust acceleration magnitude is $f=2\eta P/(mgI_{\mathrm{sp}})$, where m is the current spacecraft mass. With $\boldsymbol{y}=[\boldsymbol{x}\ t\ m]$ and $\Delta\boldsymbol{y}=[\Delta\boldsymbol{x}\ \Delta t\ \Delta m]$, the elements in the $(i+k)$th revolution are computed by using the modified Euler integration step,

$$\boldsymbol{y}_{i+k}=\boldsymbol{y}_i+\Delta\boldsymbol{y}_i \tag{25}$$

$$\boldsymbol{y}_c=(\boldsymbol{y}_i+\boldsymbol{y}_{i+k})/2 \tag{26}$$

$$\boldsymbol{y}_{i+k}=\boldsymbol{y}_i+\Delta\boldsymbol{y}_c \tag{27}$$

The value of k can be selected according to the osculating orbital period $2\pi/n$,

$$k=\begin{cases}1 & \text{if}\quad \mathrm{mod}(P_{\mathrm{ob}},2\pi/n)<1\\ \mathrm{mod}(P_{\mathrm{ob}},2\pi/n) & \text{if}\quad \mathrm{mod}(P_{\mathrm{ob}},2\pi/n)\geq 1\end{cases} \tag{28}$$

where P_{ob} is a predefined orbital period threshold value. The operator mod obtains the integer part of the real number $P_{\mathrm{ob}}/(2\pi/n)$. If P_{ob} is small or the current orbital period is large, then $k=1$, and we compute $\Delta\boldsymbol{y}$ for each orbital revolution. If P_{ob} is large or the current orbital period is small, then $k>1$, and we propagate the elements over several revolutions. The desired final semimajor axis a_f or final time t_f can be specific as the stopping condition for the orbital averaging technique. If semimajor axis is the stopping condition, then the flight time, mass, and states at a_f are obtained by linear interpolation as $a_i\leq a_f<a_{i+k}$,

$$\boldsymbol{y}_f=\boldsymbol{y}_i+\frac{a_f-a_i}{a_{i+k}-a_i}(\boldsymbol{y}_{i+k}-\boldsymbol{y}_i) \tag{29}$$

If flight time is the stopping condition, then the states and mass at t_f are obtained by linear interpolation as $t_i\leq t_f<t_{i+k}$,

$$\boldsymbol{y}_f=\boldsymbol{y}_i+\frac{t_f-t_i}{t_{i+k}-t_i}(\boldsymbol{y}_{i+k}-\boldsymbol{y}_i) \tag{30}$$

One disadvantage of the proposed orbital averaging approach is that it cannot simulate hyperbolic trajectories. Furthermore, eccentricity cannot be exactly zero or argument of periapsis and its dynamic equation are undefined.

Comparison Between Orbital Averaging and Precise Integration

Trajectories obtained by the analytic orbital averaging technique are compared with trajectories obtained by precise numerical integration methods. Several Earth-orbit raising trajectories using tangential acceleration are obtained, and in each case, the spacecraft parameters are $P = 5$ kW, $I_{sp} = 3000$ s, $\eta = 0.6$, and the initial mass is $m_0 = 1000$ kg, which results in a very low initial thrust-to-weight ratio of 2.08×10^{-5}. Table 1 presents the initial orbital elements, desired stopping condition (t_f or a_f), and period parameter P_{ob} for three simulation cases. The calendar date is fixed at 1 January 2008 for all initial orbits (required for Earth-shadow conditions). Earth-shadow periods and J_2 perturbation effects are included in all cases. Earth-shadow conditions are important for analyzing the motion of solar electric propulsion spacecraft, and the cylindrical shadow model[9] is employed. A fixed-step, fourth-order Runge–Kutta method with 500,000 steps is utilized for precise numerical integration.

Table 1 Parameters for trajectory simulations

Case	a_0, Re	e_0	i_0, rad	Ω_0, rad	ω_0, rad	θ_0, rad	Stopping condition	P_{ob}, days
1	3.82	0.731	0.2	1	2	0	$t_f = 190$ days	0
2	2.1	0.5	0.3	3	4	2	$t_f = 260$ days	1
3	1.08	0.001	0.5	5	6	1	$a_f = 70$ Re	1

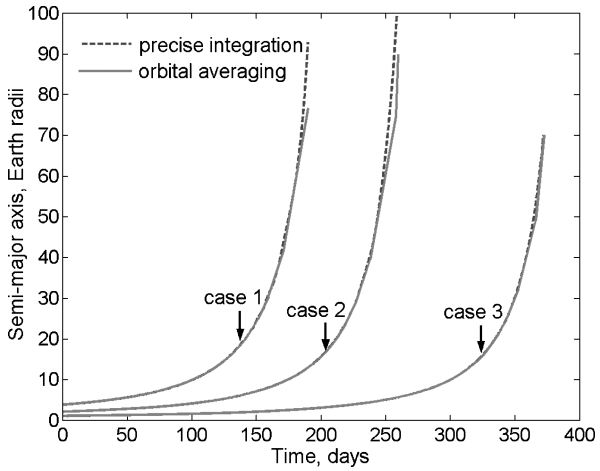

Fig. 1 Time histories of semimajor axis.

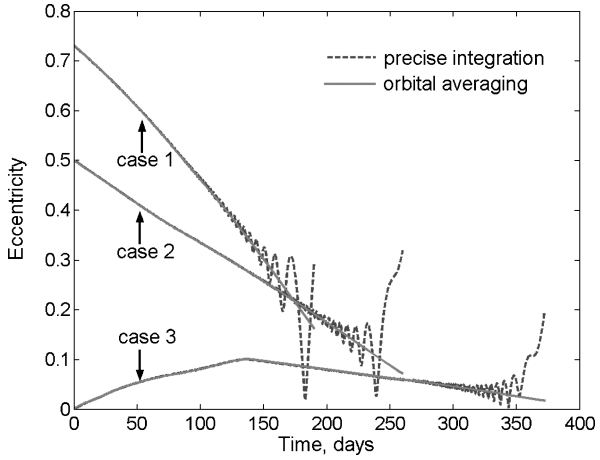

Fig. 2 Time histories of eccentricity.

Table 2 Results obtained by orbital averaging and precise integration

Case	Orbital averaging a_f Re	Orbital averaging m_f, kg	Orbital averaging t_f, days	Full integration a_f Re	Full integration m_f, kg	Full integration t_f, days
1	76.66	887.92	190	92.81	887.90	190
2	89.83	848.80	260	107.16	848.76	260
3	70	797.69	372.89	70	798.00	372.19

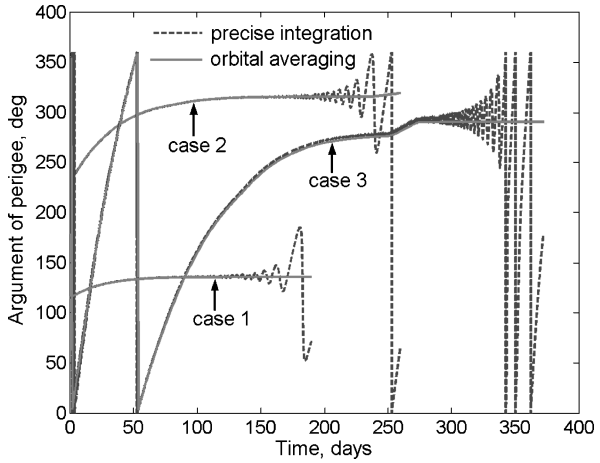

Fig. 3 Time histories of argument of perigee.

Figures 1–3 present the time histories for semimajor axis, eccentricity, and argument of perigee for the two simulation methods. Figures 1–3 demonstrate that the orbital averaging method (using the approximate analytic integrals) shows very good agreement with the precise numerical solutions. Note that the initial orbits for cases 1 and 2 have large eccentricity (Fig. 2) and that the approximate analytic integrals produce mean eccentricity profiles that track the osculating eccentricity. The averaged trajectories show good accuracy until the semimajor axis (or period) becomes too large and the assumptions for averaging break down. (In all cases, we chose to propagate the trajectories to within a few revolutions of orbital escape conditions.) It is reasonable to expect orbital averaging methods to show good accuracy up to some maximum orbital period (or semimajor axis) value, and Figs. 2 and 3 show very good accuracy for each case up to $a = 20$ Earth radii (20 Re).

Table 2 presents a summary of the simulation results obtained by orbital averaging and full numerical integration. Despite the excessive trajectory propagation to near-escape conditions, the performance parameters (final mass and trip time for case 3) show good agreement between the averaging and precise integration methods.

Conclusions

The computational burden of simulating long-duration, many-revolution planar tangential-thrust trajectories is alleviated by a new orbital averaging technique. Simple analytic expressions for the incremental changes in the classical orbital elements in presence of Earth-shadow and oblateness effects are derived. The time histories of classical orbital elements are obtained. Our new orbital averaging technique is fast and exhibits satisfactory solution accuracy when compared with precise integration results. Our method may be useful as tool for rapid performance calculations (time of flight and propellant mass), and it may be useful for simulating long-during transfers in the context of a numerical trajectory optimization program.

References

[1]Kechichian, J. A., "Orbit Raising with Low-Thrust Tangential Acceleration in Presence of Earth Shadow," *Journal of Spacecraft and Rockets*, Vol. 35, No. 4, 1998, pp. 516–525.

[2]Benney, D. J., "Escape from a Circular Orbit Using Tangential Thrust," *Jet Propulsion*, Vol. 28, March 1958, pp. 167–169.

[3]Kluever, C. A., "Optimal Earth-Capture Trajectories Using Electric Propulsion," *Journal of Guidance, Control, and Dynamics*, Vol. 25, No. 3, 2002, pp. 604–606.

[4]Perkins, F. M., "Flight Mechanics of Low-Thrust Spacecraft," *Journal of the Aerospace Sciences*, Vol. 26, May 1959, pp. 291–297.

[5]Stark, H. M., and Arthur, P. D., "Simple Approximate Solutions for Tangential, Low-Thrust Trajectories," *Journal of the Aerospace Sciences*, Vol. 28, Nov. 1961, pp. 897–898.

[6]Zee, C.-H., "Low Constant Tangential Thrust Spiral Trajectories," *AIAA Journal*, Vol. 1, No. 7, 1963, pp. 1581–1583.

[7]Sukhanov, A. A., and Prado, A. F. B. de A., "Constant Tangential Low-Thrust Trajectories near an Oblate Planet," *Journal of Guidance, Control, and Dynamics*, Vol. 24, No. 4, 2001, pp. 723–731.

[8]Battin, R. H., *An Introduction to the Mathematics and Methods of Astrodynamics*, AIAA Education Series, AIAA, New York, 1987, pp. 488, 489.

[9]Neta, B., and Vallado, D., "On Satellite Umbra/Penumbra Entry and Exit Positions," *Journal of the Astronautical Sciences*," Vol. 46, No. 1, 1998, pp. 91–104.